NASA TECHNICAL NOTE

NASA TN D-3985

NASA TN D-3985

SLOSH DYNAMICS STUDY IN NEAR ZERO GRAVITY

DESCRIPTION OF VEHICLE AND SPACECRAFT

by Harold Gold, Jack G. McArdle, and Donald A. Petrash

Lewis Research Center
Cleveland, Ohio

NATIONAL AERONAUTICS AND SPACE ADMINISTRATION • WASHINGTON, D. C. • MAY 1967

NASA TN D-3985

SLOSH DYNAMICS STUDY IN NEAR ZERO GRAVITY

DESCRIPTION OF VEHICLE AND SPACECRAFT

By Harold Gold, Jack G. McArdle, and Donald A. Petrash

Lewis Research Center
Cleveland, Ohio

NATIONAL AERONAUTICS AND SPACE ADMINISTRATION

For sale by the Clearinghouse for Federal Scientific and Technical Information
Springfield, Virginia 22151 – CFSTI price $3.00

SLOSH DYNAMICS STUDY IN NEAR ZERO GRAVITY - DESCRIPTION OF VEHICLE AND SPACECRAFT

by Harold Gold, Jack G. McArdle, and Donald A. Petrash
Lewis Research Center

SUMMARY

A spacecraft carrying a 22-inch-diameter, 44-inch-long transparent tank equipped with a slosh baffle and partially filled with alcohol was flown into a ballistic trajectory on June 7, 1966, by the two-stage WASP (Weightlessness Analysis Sounding Probe) rocket. In free flight the spacecraft was rate-stabilized by a proportional gas-jet system. Thrusts were provided that established 6.5×10^{-3}- and 7.3×10^{-4}-g acceleration along the longitudinal axis of the tank and a lateral acceleration of 7×10^{-3} g for periods of a few seconds (to induce sloshing of the alcohol within the tank). The spacecraft carried a television system for observation of the alcohol motion. The damping induced by the slosh baffle was sufficient to damp slosh in less than one-quarter cycle at both longitudinal accelerations. The performance of the WASP vehicle, which provided a period of over 6 minutes of flight above an altitude of 250 000 feet for the 1528-pound payload, was very close to design values on this, its first, flight test.

INTRODUCTION

The Project WASP (Weightlessness Analysis Sounding Probe) experiment reported herein was part of the NASA study of the control of liquid location in partially filled tanks during coasting flight. This program was undertaken because the mission capability of rocket booster stages for orbital and interplanetary flight can be significantly increased through the use of alternate periods of thrust and coast. With rocket stages that employ cryogenic propellants, locating the liquid at the pump inlet end of the tank during coast permits gaseous venting by simple means. This also is essential for engine restart for both cryogenic and storable propellants.

The WASP experiment was performed as a part of an overall research program investigating the scaling of low-gravity phenomena applicable to the method of liquid location during coast that is currently being used on the NASA Saturn and Centaur vehicles. This method employs low-level longitudinal thrusts that produce forward acceleration in the range 10^{-3} to 10^{-6} g. These acceleration levels were determined from drop-tower experiments (ref. 1).

Visual data were obtained to determine the time required to reorient a liquid to the low-gravity configuration after the liquid turbulence that may follow cutoff of vehicle thrust and to evaluate the effectiveness of a ring-type baffle in suppressing slosh in low gravity. The experiment was performed with a 22-inch-diameter, 44-inch-long transparent tank and with alcohol as a liquid-hydrogen simulator. Continuous longitudinal thrust and short periods of slosh-inducing lateral thrust were provided. The liquid motion was observed through television cameras which viewed the tank from the side along an optical axis that was essentially perpendicular to the lateral thrustor. The tank was carried aboard a spacecraft that was placed in a ballistic trajectory which resulted in approximately 6 minutes of experiment time.

The rocket vehicle employed was a two-stage sounding rocket that was designed for Project WASP. The rocket carried a total payload-and-spacecraft-housing weight of approximately 1500 pounds on this, its first, flight. The rocket was launched from the NASA Wallops Island Station on June 7, 1966.

This report presents a description of the spacecraft and rocket vehicle and those significant results of the liquid dynamics phenomena and of the spacecraft and vehicle performance that could be interpreted without detailed analysis. Descriptive information and performance data on important details of the vehicle and spacecraft are included as a contribution to sounding-rocket and spacecraft technology.

CONFIGURATION OF VEHICLE AND SPACECRAFT

Launch Configuration

An outline drawing of the WASP vehicle with the nose cone attached is shown in figure 1. The vehicle employed two solid-propellant stages, both of which were stabilized aerodynamically and through vehicle spin. The first-stage motors were the XM33E6 Pollux and two XM19E1 Recruits, and the second-stage motor was an X259-A2 Antares. Fin cant was used to induce vehicle spin. A photograph of the vehicle and the payload assembly mounted on the vehicle launcher is presented in figure 2. An illustration of the spacecraft within the housing is shown in figure 3. The spin isolator, identified in figure 3, prevented rocket spin from being transmitted to the spacecraft. The total weight of the WASP spacecraft, the housing, and the spin isolator was 1528 pounds.

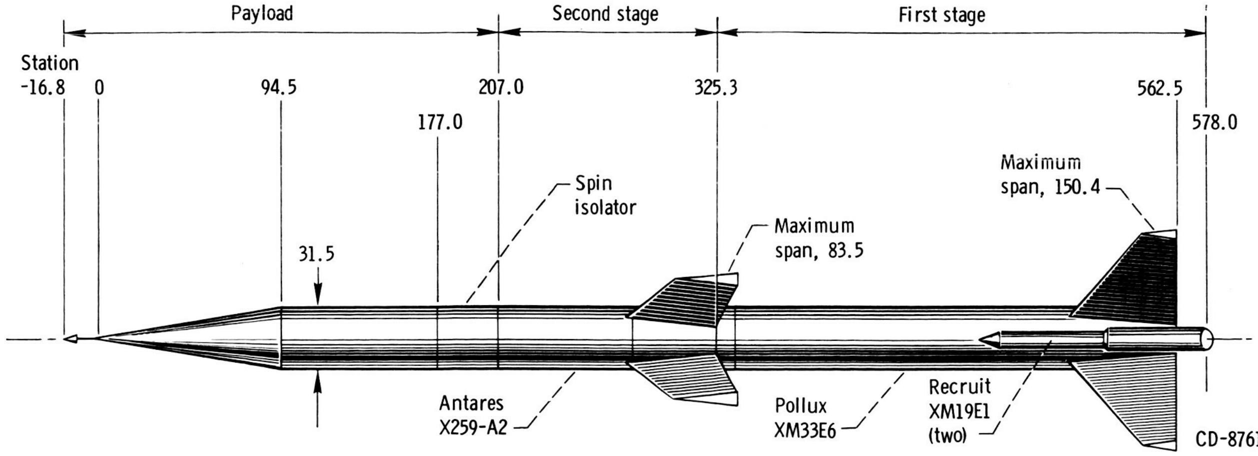

Figure 1 - WASP vehicle with nose cone attached. (Dimensions in inches.)

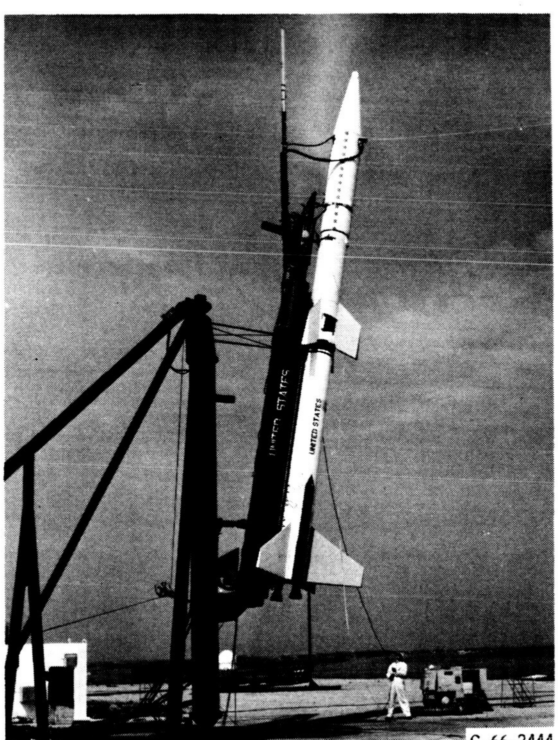

Figure 2. - WASP vehicle on launcher at NASA Wallops Station, Wallops Island, Virginia

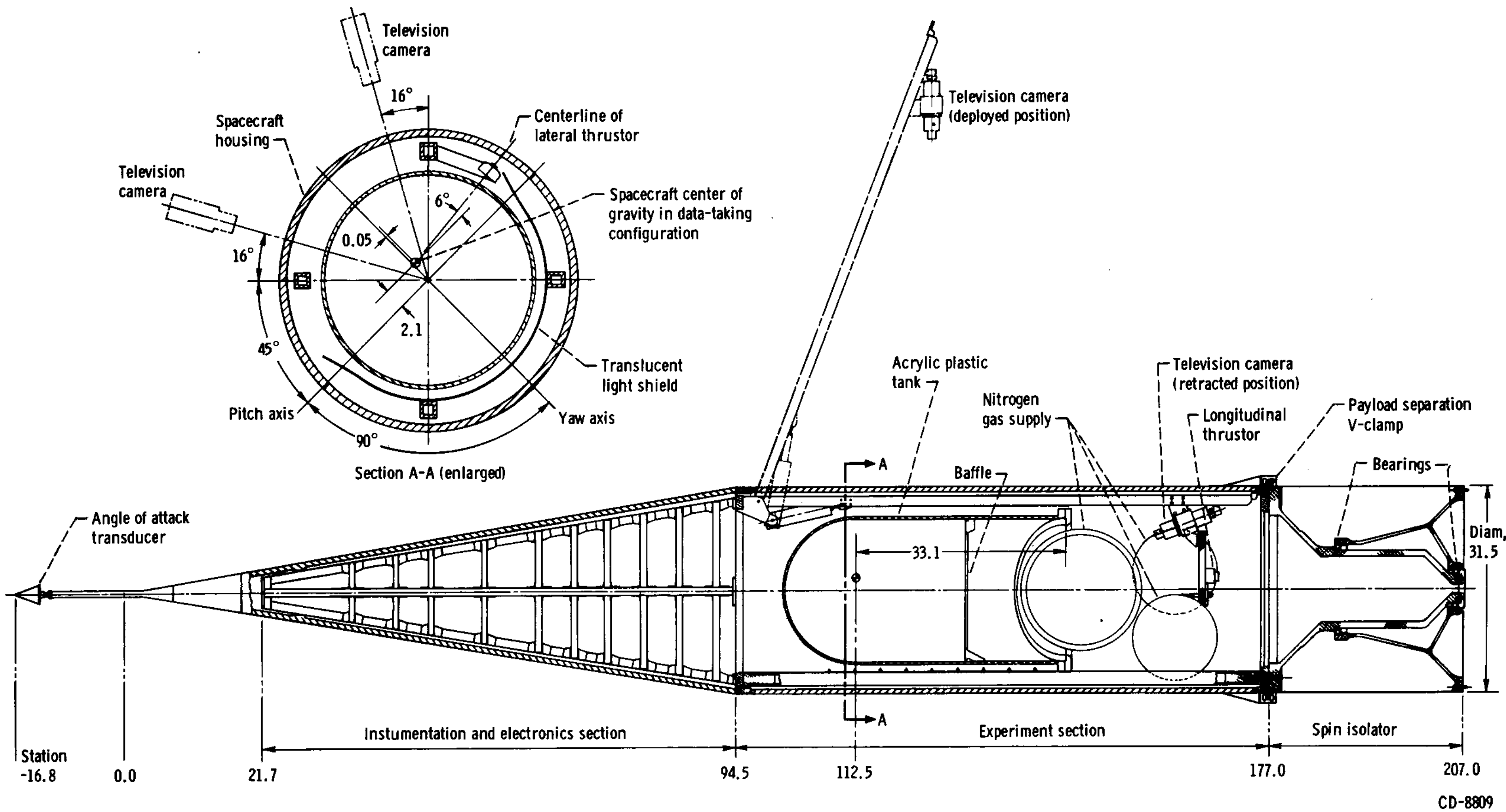

Figure 3. - Sketch of WASP Spacecraft for low-g slosh-dynamics flight test, with housing and spin isolator. Most supporting structure, bracketry, and electrical components omitted to improve clarity. (Dimensions in inches or degress as appropriate.)

Free-Flight Configuration

After the payload was separated from the spin isolator, the housing was jettisoned by being split into two longitudinal sections. This action exposed the transparent tank to sunlight and permitted the hinged arms that carried the television cameras to move outward.

The deployed positions of the television cameras are illustrated in figure 3. As indicated in section A-A of figure 3, a translucent shield covered the back of the transparent tank to shield the television cameras from direct sunlight.

A nitrogen jet located at the base of the spacecraft provided the longitudinal settling thrust. A second jet located on the side of the spacecraft and thrusting through the center of gravity along a line essentially perpendicular to the optical axes of the cameras provided the lateral disturbing thrust (see section A-A, fig. 3).

In free flight, the spacecraft was stabilized by a proportional, pneumatic, rate-damping system.

The weight of the spacecraft in free-flight configuration was 862 pounds, including 95 pounds of alcohol in the transparent tank and full pressure in the nitrogen storage tanks.

DESCRIPTION OF VEHICLE

First Stage

The WASP first stage was the same as the first stage of the Shot-Put sounding rocket (ref. 2), with the exception of the structure and the mechanism used for second-stage coupling. The Pollux sustainer motor burned for approximately 25 seconds at an average sea level thrust of about 50 000 pounds, with an additional 8-second thrust decay to burnout. The added thrust of the Recruit boosters provided the vehicle with a lift-off thrust of approximately 130 000 pounds. The total Recruit burning time was approximately 2.5 seconds. The four first-stage fins were 8° wedges with a maximum span of 150.4 inches and a unit planform area of 15 square feet. The nominal first-stage lift-off and burnout weights were 10 282 and 2602 pounds, respectively.

Second Stage

A V-clamp joined the second-stage fin structure to the thrust structure of the first stage. The four second-stage fins were 10° wedges with a maximum fin span of 83.5

inches and a unit planform area of 7.5 square feet. The Antares motor was insulated against aerodynamic heating by a fiber-glass blanket and an outer aluminum sheet fairing. The second-stage thrust structure was joined to a 12-inch-long payload adapter by a V-clamp. The adapter terminated at a tapped hole flange. Second-stage ignition was initiated by a timer started at lift-off. The Antares motor burned for approximately 30 seconds at an average vacuum thrust of approximately 22 000 pounds, with an additional 4-second thrust decay to burnout. The nominal second-stage initial and final weights were 3277 and 687 pounds, respectively.

Spin Isolator

The platform of the spin isolator was rate-controlled to prevent the payload from spinning during rocket boost. The isolator was driven by a hydraulic motor. Power was provided by an electric-motor-driven hydraulic pump, and speed was modulated through an electrohydraulic servovalve. The error signal from the spin isolator rate-gyro was fed into a proportional-plus-integral control amplifier, the output of which drove the servovalve. A photograph of the spin isolator showing the drive mechanism is presented in figure 4. The isolator was 30 inches long and weighed 350 pounds. It was bolted to the second-stage payload adapter. The spacecraft with the housing was fastened to the isolator platform by a V-clamp. The isolator could compensate for rocket spin rates up to 6 rps.

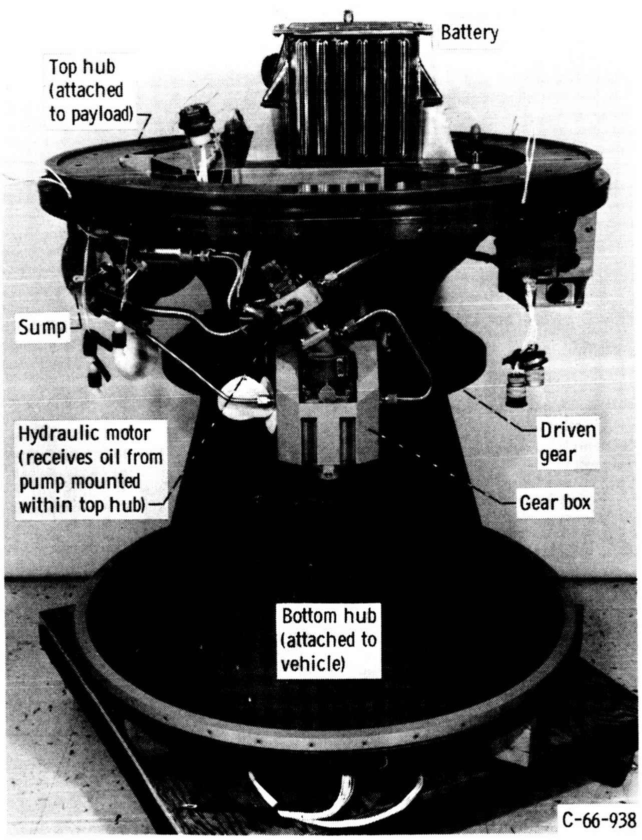

Figure 4. - Spin isolator.

Spacecraft Housing

The overall dimensions of the spacecraft housing are shown in figure 3 (p. 4). It consisted of a cylindrical section and a conical section, which were joined by screws. Both sections were constructed of a filament-wound fiber-glass honeycomb sandwich material. The honeycomb material for each section was formed into two longitudinal, semicircular segments that were cemented to longitudinal frangible fiber-glass blocks. The blocks were drilled through their entire length to accept a continuous loop of primacord. The spacecraft housing was fastened to the spin isolator platform by a V-clamp. The housing in turn clamped the spacecraft to the platform. Internal aluminum rings, which were cemented in the housing at the top of the cylindrical section and at the top of the conical section, provided lateral support points for the spacecraft.

The spacecraft and housing were released, as a unit, from the spin isolator by firing four explosive bolts in the V-clamp. After release, springs imparted a 2-foot-per-second longitudinal separation velocity. Two seconds after release, the primacord in the spacecraft housing was fired. This caused the housing to break into halves and propelled them radially away from the spacecraft.

TABLE I. - BOOST EVENT SEQUENCE

Nominal time from launch, sec	Event
2.5	Recruit burnout
33.0	First-stage burnout
35.0	Second-stage separation
38.7	Second-stage ignition
72.7	Second-stage burnout
95.0	Payload separation
97.0	Spacecraft housing separation

Boost-Phase Sequence

The boost-phase timing sequence and approximate burnout times are presented in table I. The 22.3-second delay between second-stage burnout and payload separation was incorporated to assure complete thrust decay of the second-stage motor.

DESCRIPTION OF SPACECRAFT

Structure

As illustrated in figure 3 (p. 4), the spacecraft comprised a conical instrumentation and electronics section and a cylindrical experiment section. Figure 5 (p. 8) is a photograph of the spacecraft taken during a center-of-gravity determination. The experiment-section structure consisted of four longitudinal posts of extruded square-section aluminum. The posts were bolted to upper and lower aluminum rings. Milled square sections that projected from the rings and inserted into the extruded posts provided the bolting interface. The transparent tank and the gas storage spheres were mounted from the posts. The camera-arm-hinge and actuator assemblies were fastened to the upper ring of the experiment section. The instrumentation and electronics section was constructed

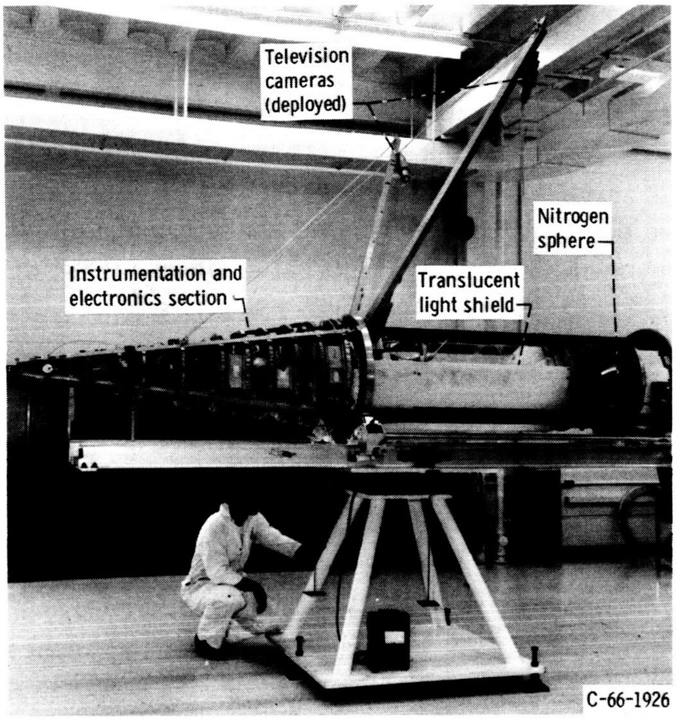

Figure 5. - Project WASP spacecraft for low-g slosh-dynamics flight test.

of extruded square-section aluminum longitudinal members and honeycomb aluminum trays. The trays were fastened to the longitudinal members by bolted brackets.

Camera Actuators

The camera actuators were spring driven and hydraulically damped. The springs were contained in the damper cylinder, and the spring force was transmitted through the damper piston and the output shaft. The actuators were linked to their camera arms in a rocking-cylinder configuration. The ends of the camera arms were restrained against the structure by the spacecraft housing. Following housing separation, the rate of camera deployment was controlled by an orifice across the damper piston. The orifice was automatically closed at the end of piston travel to limit end shock. The two actuators were mechanically and hydraulically independent. The deployment time was 4 seconds, and the end shock was 2 g's.

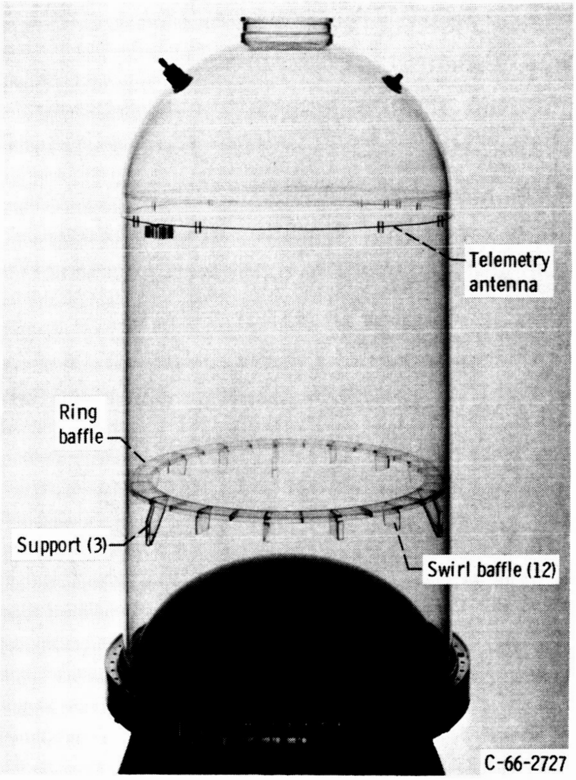

Figure 6. - Tank and baffle used in Project WASP low-g slosh-dynamics flight test.

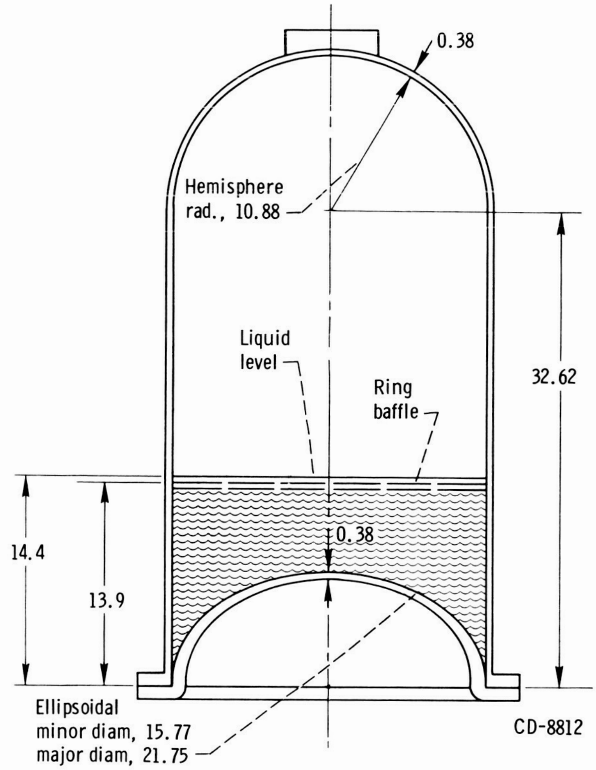

Figure 7. - Tank and baffle configuration. (Dimensions in inches.)

Transparent Tank and Test Liquid

A photograph of the tank is given in figure 6, and the principal dimensions and configuration of the tank are shown in figure 7. The tank was fabricated from acrylic plastic. The baffle parts were machined from acrylic plastic sheet and cemented to the tank wall.

The test liquid was 200-proof anhydrous ethanol to which a small amount of dye had been added to improve the photographic quality. The addition of the dye had no measurable effect on the physical properties of the liquid. The 95 pounds of alcohol required to fill the tank to 1/2 inch above the top of the baffle was loaded at atmospheric pressure. The tank remained unvented throughout the flight.

Propulsion System

The longitudinal-thrust and lateral-thrust propulsion systems utilized nitrogen gas as the propellant. The gas supply was contained in two spherical fiber-glass tanks, one 21 inches in diameter and one 10 inches in diameter, joined to a common outlet line and pressurized to 3000 psia. A nozzle located at the bottom of the spacecraft and thrusting through the center of gravity provided the longitudinal thrust. This nozzle developed two levels of thrust: 6 and 0.8 pound. These values were selected to produce approximately 7×10^{-3}- and 9×10^{-4}-g acceleration of the 862-pound spacecraft. For the lower thrust level there was a fixed flow restriction between the nozzle and the pressure regulator. This restriction was bypassed by a solenoid valve for the higher thrust level. The lateral nozzle was located near the top of the experiment section and acted through the spacecraft center of gravity along a line nearly perpendicular to the line bisecting the camera angle (see fig. 3, p. 4). This lateral thrustor produced 6 pounds of thrust and was controlled by a solenoid valve. A series regulator close to each nozzle held the nozzle inlet pressure at approximately 130 psia.

Rate-Damping System

A photograph of the three-axis orthogonal rate-gyro assembly mounted on its supporting electronic package is presented in figure 8. The electronic package contained the inverter, demodulators, amplifiers, and associated electronic components. The amplifier outputs of the gyro-signal demodulators were used to drive pneumatic, proportional, spool-type four-way valves. Each of the two output ports of each four-way valve was connected to a separate nozzle to provide bidirectional torque about each axis. Torque was applied about the roll axis by a two-nozzle pair and about the pitch and yaw axes

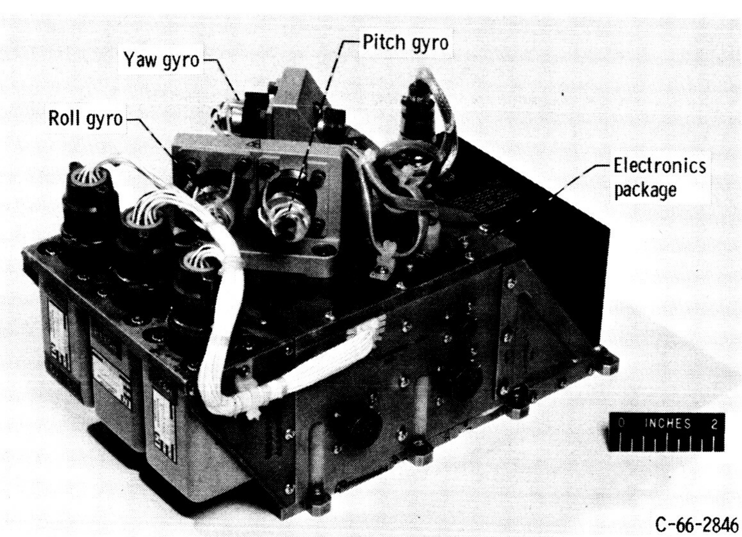

Figure 8. - Rate gyro assembly on electronics package.

through single-nozzle pairs. Nitrogen was supplied from one 10-inch fiber-glass spherical tank pressurized to 3000 psia. The gas pressure at the four-way valves was held at 900 psi by a series regulator.

Instrumentation and Telemetry

Telemetered information included data on rocket and spacecraft performance as well as on the slosh dynamics experiment. Rocket acceleration, first- and second-stage motor pressures, and boost vibration levels were transmitted. The spin-isolator platform provided the rocket spin-rate reference; the rotation rate of the spin isolator was detected by the roll-axis rate gyro of the rate-damping system. Critical hydraulic pressures and control system voltages in the spin isolator were monitored.

On the spacecraft, the free-flight longitudinal acceleration, attitude rates, and longitudinal- and lateral-nozzle inlet pressures were measured. The longitudinal accelerometer had a threshold of 10^{-5} g and a full-scale value of 10^{-2} g. The accelerometer output was transmitted on two telemeter channels: one $\pm 10^{-3}$ g (full scale) and the other $\pm 10^{-2}$ g. The rate gyros of the rate-damping system provided three-axis rate information with a threshold of 0.01° per second and a full-scale value of approximately 3.6° per second. Nozzle inlet pressures were measured through 200-psia full-scale transducers. The telemetry system was FM/FM, conforming to the Interrange Instrumentation Group (IRIG) standards, and utilized subcarrier channels 1 to 18. The telemetry transmitting frequency was 240.2 megahertz, and the output power was 10 watts. The telemetry transmitting antenna was a circular dipole that was mounted on the cylindrical wall of the transparent tank perpendicular to the cylindrical axis.

The two television systems conformed to the specifications given in table II. The low- and the high-voltage circuits had independent switches to permit prelaunch and boost-phase warmup and high voltage (500 V) turnon after spacecraft separation. Each television transmitter was connected with a circumferential slot antenna, one of which was integrated into the lower-tank support structure and the other into the 21-inch-sphere support structure.

TABLE II. - TELEVISION SYSTEM SPECIFICATIONS

Type of modulation	Video/FM
Center frequency, Mhz	
System 1	225.0
System 2	250.5
Bandwidth, MHz	±5
Maximum output power, W	23
Horizontal sweep rate, Hz	15 750
Framing rate, frames/sec	30
Field rate (with 2 to 1 positive interlace), Hz	60
Video bandwidth, MHz	8
Horizontal and vertical sweep linearity, percent	±2

Experiment Event Sequence

For the experiment, the spacecraft electromechanical programer was set for the sequence of events listed in table III.

TABLE III. - PROGRAMED EVENT SEQUENCE

Event number	Nominal time from launch, sec	Event
1	100	Six-pound-longitudinal-thrustor turnon
2	160	Lateral-thrustor turnon
3	165	Lateral-thrustor turnoff
4	240	Longitudinal-thrust reduction to 0.8 lb
5	258	Lateral-thrustor turnon
6	262	Lateral-thrustor turnoff

Command System

A ten-channel frequency-modulation command-receiver decoder was utilized to back up the onboard programer and to permit variation in the programed event sequence. The command system capability was as follows:

(1) Programer backup:

(a) Payload separation (95 sec after lift-off)

(b) Spacecraft-housing jettison (97 sec after lift-off)

(c) Propulsion system activation (98 sec after lift-off)

(d) Rate-damping system activation (98 sec after lift-off)

(e) High-voltage television systems turnon (98 sec after lift-off)

(2) Programer override:

(a) Lateral-thrustor turnon

(b) Lateral-thrustor turnoff

(c) Longitudinal thrust reduction to 0.8 pound

(d) Longitudinal thrust increase to 6 pounds

(e) Rate-damping system disabling

(f) High-voltage television systems turnon

(g) High-voltage television system (number 1) turnoff

(h) High-voltage television system (number 2) turnoff

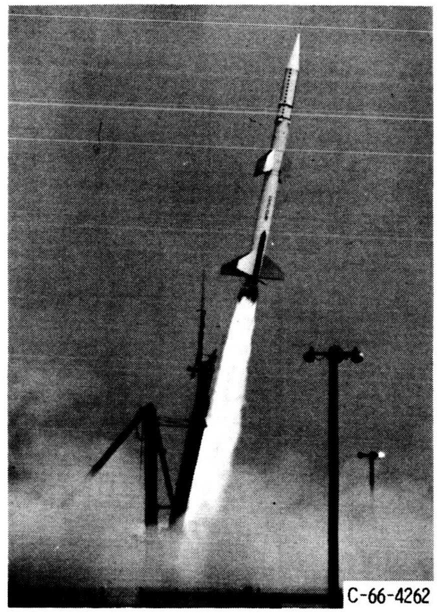

Figure 9. - Launch of WASP sounding rocket at NASA Wallops Station.

RESULTS

Vehicle Performance

Launch conditions. - The WASP rocket was launched into a clear sky from Wallops Station, Virginia, on June 7, 1966, at 11:57 a.m. e.s.t. A photograph of the launch is shown in figure 9. The average weighted wind, measured by balloons just before and just after launch, was 21.4 feet per second from 226^{o} from north. Final launcher settings, determined from James method curves (ref. 3), were 77.7^{o} elevation and 85.0^{o} azimuth.

Trajectory. - Vehicle performance for no wind and nominal conditions was predicted by using a six-degree-of-freedom trajectory-simulation program. The actual vertical and horizontal trajectories were obtained from skin-track-radar plotboard data. The predicted and actual vertical trajectories, with significant event times, are compared in figure 10(a) (p. 14) and in table IV (p. 15). Although the burnout attitude appeared to be higher than expected, the apogee altitude and total flight time are slightly less. The reasons for these differences are being investigated. The vehicle did, however, provide 6 minutes of flight above an altitude of 250 000 feet for the payload.

The horizontal trajectory (fig. 10(b)) indicates that the launcher correction in azimuth was not sufficient for the prevailing southwest winds. However, surface impact was well within the predicted 3-sigma dispersion area.

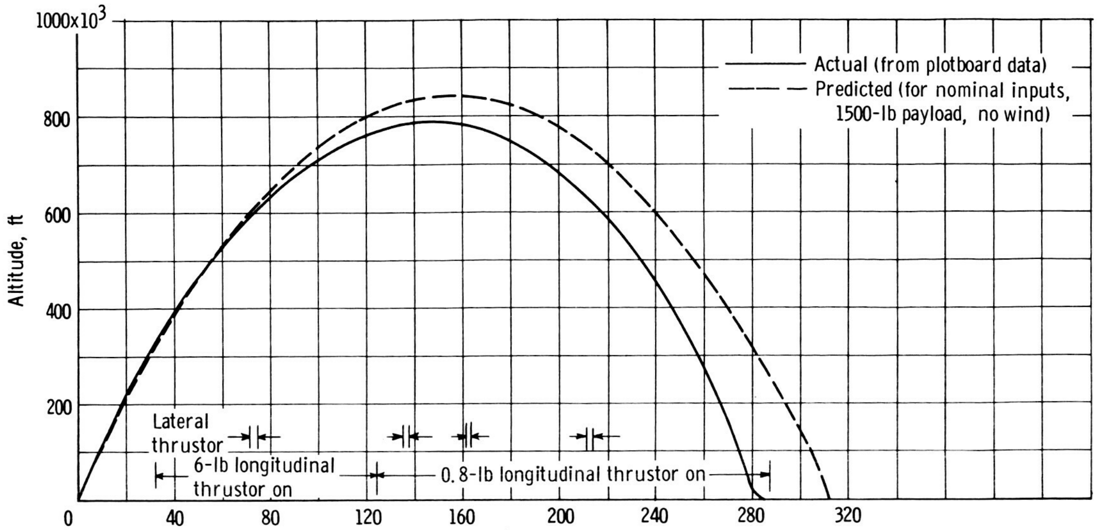

(a) Vertical trajectory.

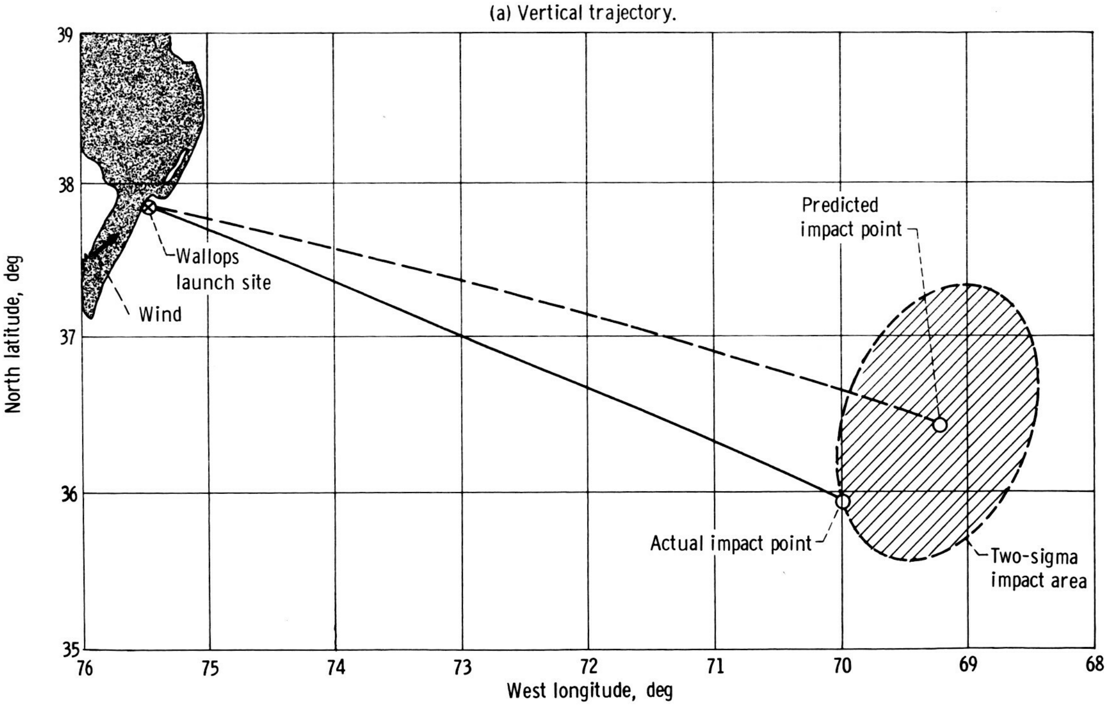

(b) Horizontal trajectory.

Figure 10. - Vehicle performance for 80° effective launch elevation.

TABLE IV. - PREDICTED AND ACTUAL VEHICLE PERFORMANCE

Event	Time from lift-off, sec		Altitude, ft	
	Predicted	Actual (a)	Predicted	Actual
Recruit burnout	2.5	2.5	0.65×10^3	---------
Staging	35.0	35.4	50.2	46.0×10^3
Antares ignition	38.7	38.5	57.0	51.0
Antares burnout	72.7	74.7	188	180
250 000-ft crossing	83.0	87.0	----------	---------
Payload separation	95.0	95.0	318	305
Apogee	286	280	842	788
250 000-ft crossing	489	465	----------	---------
50 000 ft impact	615	580	----------	---------

[a]Obtained from radar and miscellaneous vehicle performance instrumentation.

Loads. - Preflight static and dynamic structural analyses showed that the WASP-vehicle design was adequate to withstand all expected loads during ground handling and in flight with wind gusts up to 30 feet per second. The boost-acceleration history is presented in figure 11 (p. 16). As was expected, highest loading occurred during Recruit burning. Drag loading occurred during Pollux tailoff and staging, as indicated by negative acceleration.

Angle of attack was obtained in flight through a sting-mounted transducer (fig. 3, p. 4). The transducer was mounted with an alinement uncertainty of $\pm 1/2^\circ$. The average angle of attack was approximately 5° at Recruit burnout, after which it decreased rapidly to 1° and remained at approximately 1° throughout the atmospheric portion of the flight.

Shock and vibration. - Preliminary analysis of the data from vibration sensors indicated that the spacecraft was subjected to the most severe vibration environment during the transonic portion of the launch. During this period the indicated root-mean-square vibration level was approximately 4.5 g's over a bandwidth of 300 to 500 hertz. A shock of 11 g's was measured at lift-off and pyrotechnic shock at spacecraft housing deployment saturated the 20-g sensor.

Spin isolator. - The spin rate that was transmitted to the spacecraft through the spin isolator, as monitored by the roll-rate gyro of the rate-damping system, is presented in figure 12(a) (p. 16). The limit of this rate gyro was 3.6° per second. This rate was exceeded for approximately 15 seconds of the 95-second period of operation. The measured and predicted rocket spin-rate histories are shown in figure 12(b). At payload

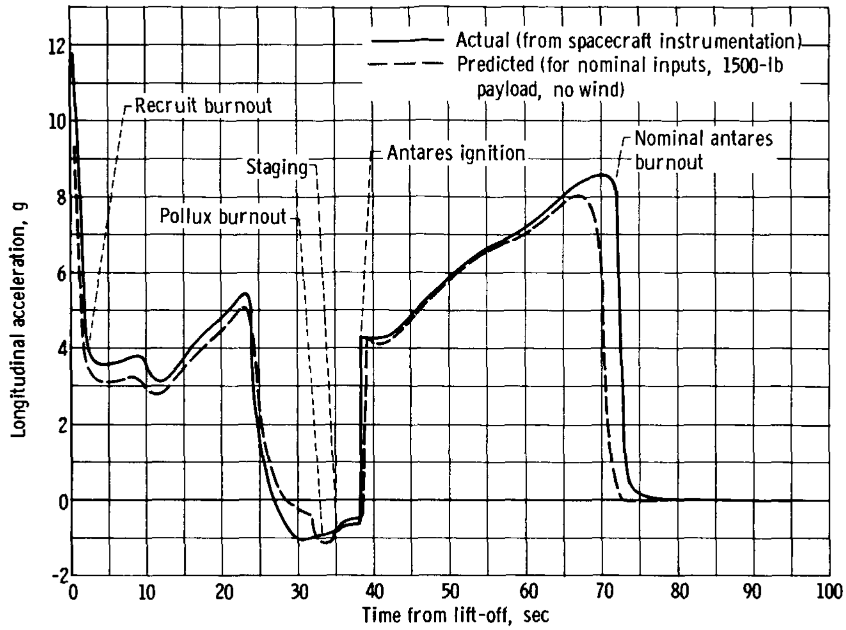

Figure 11. - Longitudinal acceleration during boost flight.

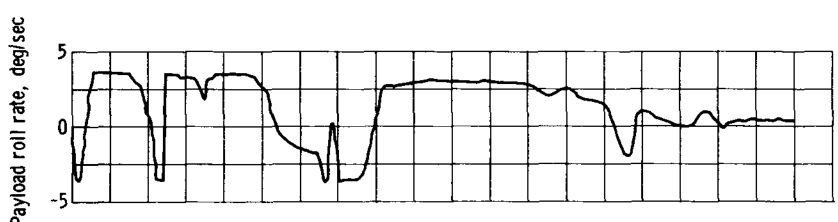

(a) Spin rate transmitted to spacecraft through spin isolator.

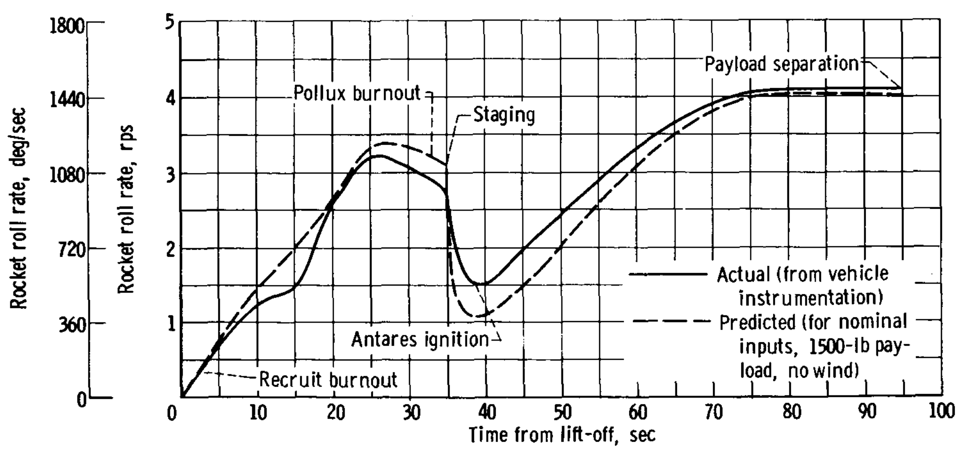

(b) Vehicle spin rate.

Figure 12. - Spin-isolator performance.

separation, the rocket spin rate was 1460° per second and that of the payload was 0.5° per second. All telemetered electrical and hydraulic spin-isolator measurements indicated normal operation throughout the flight.

Spacecraft housing. - The payload was separated from the spent second-stage rocket 95 seconds after lift-off. The primacord (10 grains per foot of length) in the housing was fired at 97 seconds after lift-off. The outward motion of the television camera arms, which followed housing jettison, was observed in the first television picture sequence. No portion of the housing nor any flying debris could be seen.

Spacecraft Performance

Rate-damping system. - The rate-damping system was activated 1 second after the spacecraft housing was jettisoned. At that instant, the combined effects of payload separation and the jettisoning of the housing produced rates of approximately 3.6° per second in roll, 0.6° per second in pitch and greater than 3.6° per second in yaw (fig. 13, p. 18). These rates initially were reduced by the rate-damping system but then were increased after 2 seconds by camera-arm deployment and again 4 seconds later by an apparent collision with the vehicle second stage. Ten seconds after rate-damping-system activation all rates were reduced below 0.1° per second. Figure 13 presents the rate gyro and longitudinal accelerometer signals over this period. The simultaneity of the rate gyro and longitudinal acceleration disturbances during this period is clearly evident. The oscillation that appeared in the roll-rate-gyro signal at each of the two disturbances corresponds in frequency with the lateral cantilever frequency of the camera arms; the lower frequency of oscillation in the accelerometer signal corresponds with the longitudinal cantilever frequency of the camera arms. Throughout the remainder of the flight, all rates were maintained below 0.1° per second, except during lateral thrustor firing, when the yaw rate increased to 0.3° per second.

Propulsion system. - The longitudinal thrustor was turned on, as programed, 100 seconds after launch. From that time until 240 seconds after launch, the longitudinal-thrustor nozzle-inlet pressure remained constant at 128 pounds per square inch absolute and produced, based on vacuum-chamber calibration, 6.0 pounds of thrust. At 240 seconds after launch, the inlet pressure and the thrust were reduced, as programed, to 19 pounds per square inch absolute and 0.8 pound, respectively. The lateral-thrustor nozzle-inlet pressure was 140 pounds per square inch absolute at each turnon and produced, based on vacuum-chamber calibration, 6.2 pounds of thrust.

Longitudinal acceleration. - Comparison of the acceleration indicated by the longitudinal accelerometer with the values calculated from the longitudinal-thrustor nozzle-inlet pressure data shows good agreement during the high-thrust period. The values

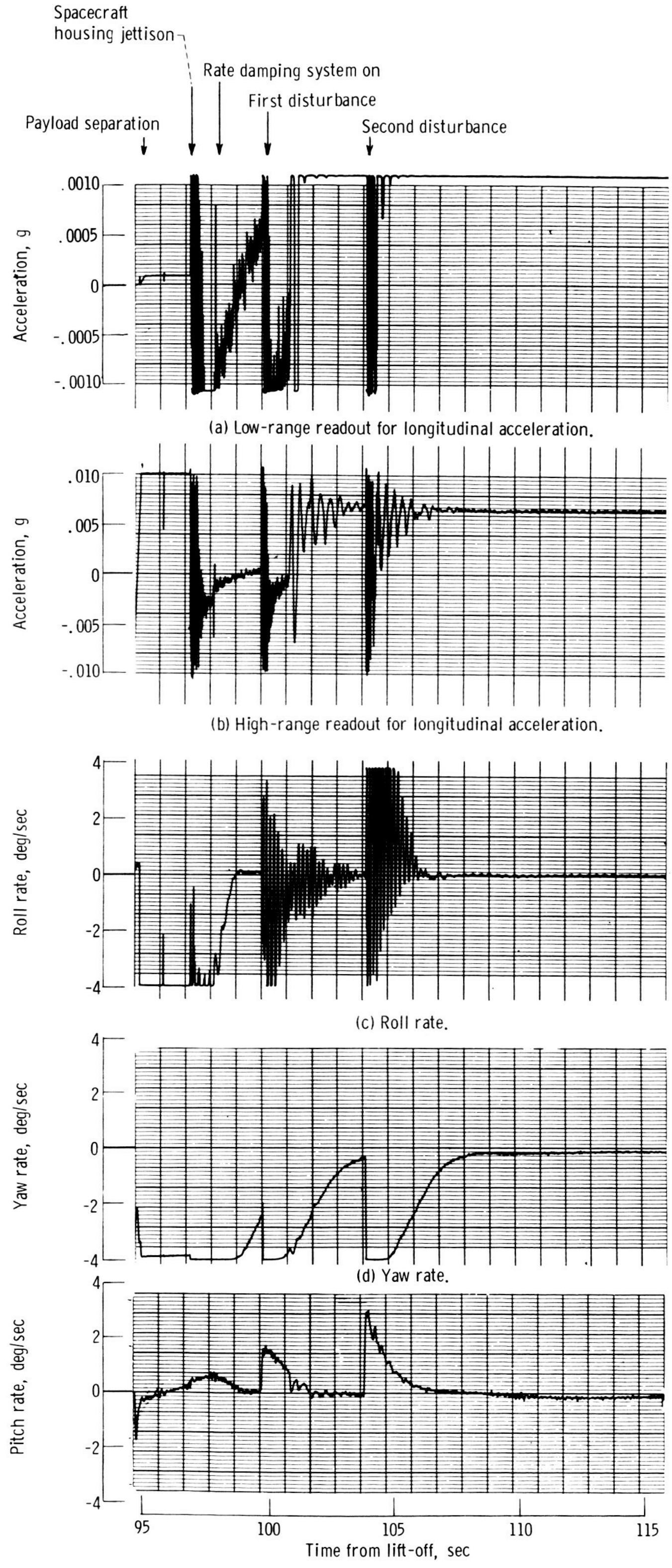

Figure 13. - Rate-gyro and spacecraft free-flight accelerometer data just after payload separation.

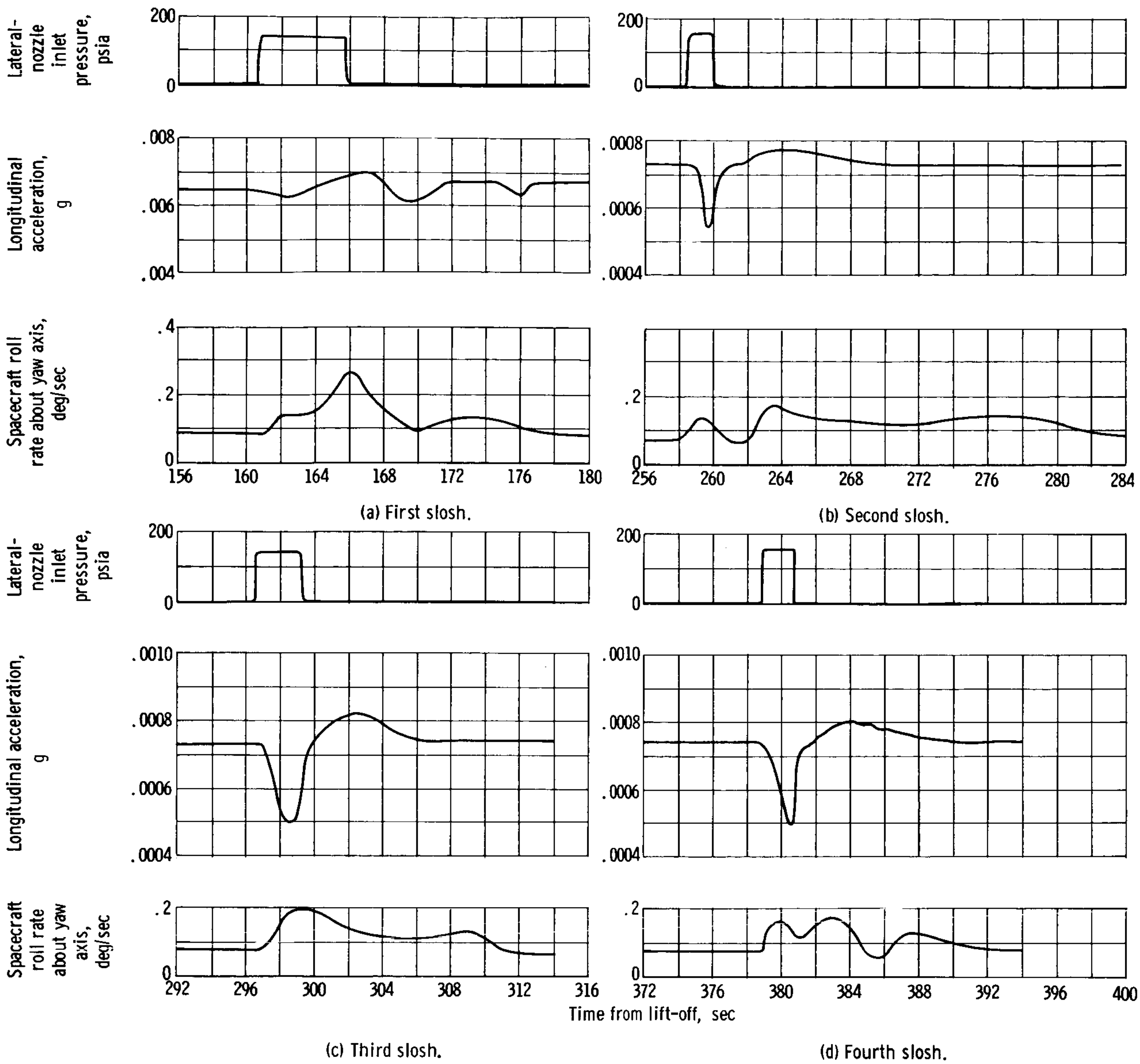

Figure 14. - Spacecraft free-flight accelerometer, yaw-rate gyro, and lateral-nozzle pressure data during sloshing.

are: 6.96×10^{-3} g (calculated) and 6.50×10^{-3} g (indicated). The acceleration values used in the analysis of the slosh dynamics are the accelerometer measurements. During the sloshing period following each application of lateral thrust, the longitudinal accelerometer indicated an oscillation. This perturbation in accelerometer data during lateral thrusting is shown in figure 14 (p. 19) along with the thrustor-nozzle-inlet pressures and the rate-gyro signals. The yaw rate, which is attributable to lateral-thrustor misalinement, could induce centrifugally approximately 10 percent of the perturbation that is seen in the accelerometer data. Therefore, the accelerometer data indicate the longitudinal-acceleration oscillation of the spacecraft that was induced by the alcohol slosh and are indicative of the overdamped slosh response that was observed in the television pictures.

Instrumentation and telemetry. - Reception of all radio signals from the spacecraft was degraded by failure of the ground-station automatic-antenna tracking system at 30 seconds after launch. After 30 seconds from launch and through the remaining flight period, emergency manual tracking was employed. The operator monitored the 240.2-megahertz carrier and attempted to hold maximum signal strength. This technique yielded the widely varying signal strength presented in figure 15. However, there was no loss of audio-range telemetered information during the flight. All instrumentation functioned normally.

Video information was received by the same antenna and was therefore severely degraded by low signal levels. During the periods of unusable video quality there was

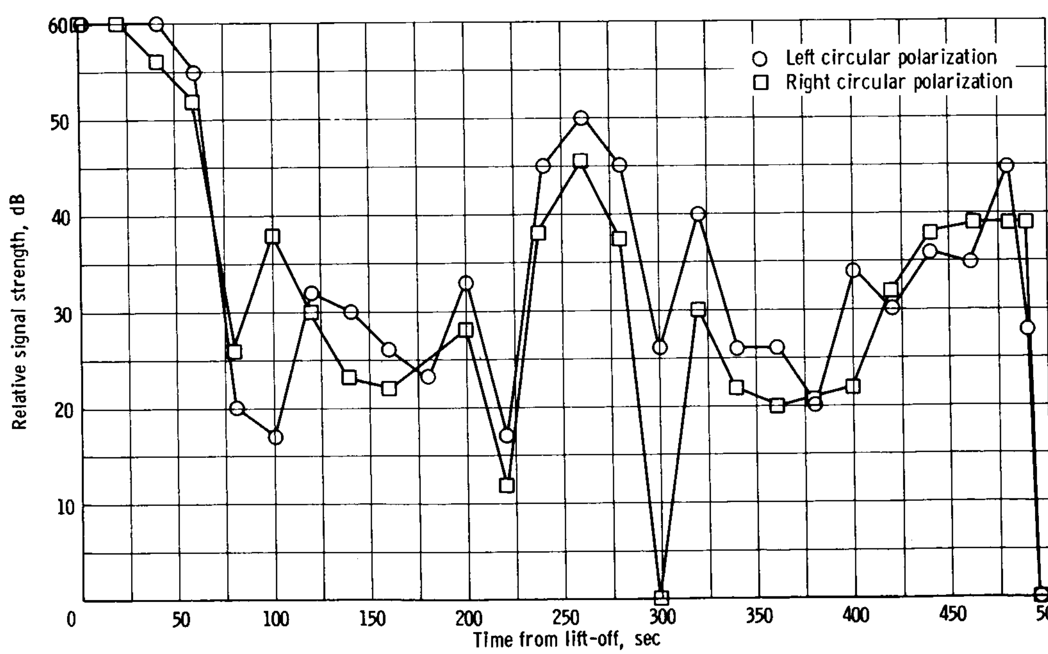

Figure 15. - Variation in telemetry signal strength during flight. Signal strength referenced to 1 microvolt at receiver input terminus (50 ohms).

severe picture distortion and loss of synchronization. However, by controlling the lateral thrustor through the ground command system, periods of adequate television signal strength were used to obtain sufficient photographic data on slosh phenomena. The flight objectives of the television system were thereby attained.

Observation of Liquid Behavior

Experiment sequence. - The onboard programer initiated events 1 to 5 of table III (p. 12). The time between events 5 and 6 was shortened to 2 seconds by terminating the lateral thrust through ground command. Two additional periods of lateral thrust were also initiated by ground command. The complete experiment sequence, both commanded and programed, is shown in table V.

TABLE V. - EXPERIMENT EVENT SEQUENCE

Event number	Nominal time from launch, sec	Event
1	100	Six-pound-longitudinal-thrustor turnon
2	160	Lateral-thrustor turnon
3	165	Lateral-thrustor turnoff
4	240	Longitudinal-thrust reduction to 0.8 lb
5	258	Lateral-thrustor turnon
[a]6	260	Lateral-thrustor turnoff
[a]7	297	Lateral-thrustor turnon
[a]8	300	Lateral-thrustor turnoff
[a]9	378	Lateral-thrustor turnon
[a]10	381	Lateral-thrustor turnoff

[a]Commanded.

Liquid reorientation. - Considerable turbulence was present in the alcohol immediately following payload separation and spacecraft housing jettison. Television frames that illustrate the nature of the turbulence are shown in figures 16(a) and (b) (p. 22). Sketches showing liquid location are included with each photograph. It is estimated that 50 percent of the alcohol was not at the bottom of the tank but was displaced at the top and along the walls. Under the longitudinal acceleration of 6.5×10^{-3} g, the liquid drained down the tank walls and was completely settled at the bottom of the tank after longitudinal thrust had been applied for approximately 30 seconds. For the remaining 30 seconds following event 1, the liquid remained at the bottom of the tank with the liquid-vapor interface quiescent and flat (fig. 16(c)).

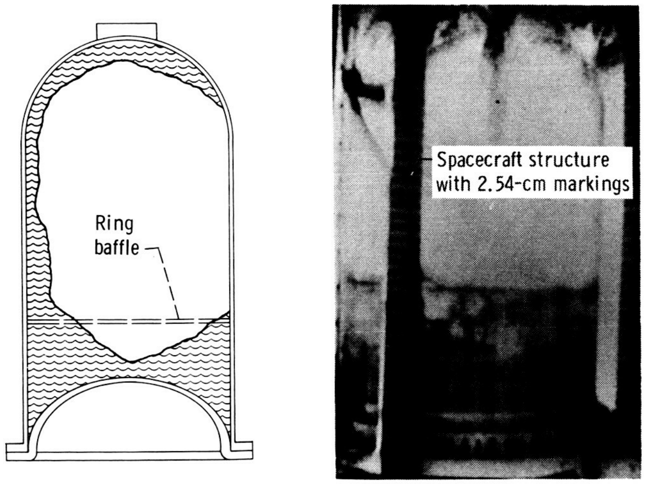

(a) Start of turbulent motion with some liquid already at top of tank.

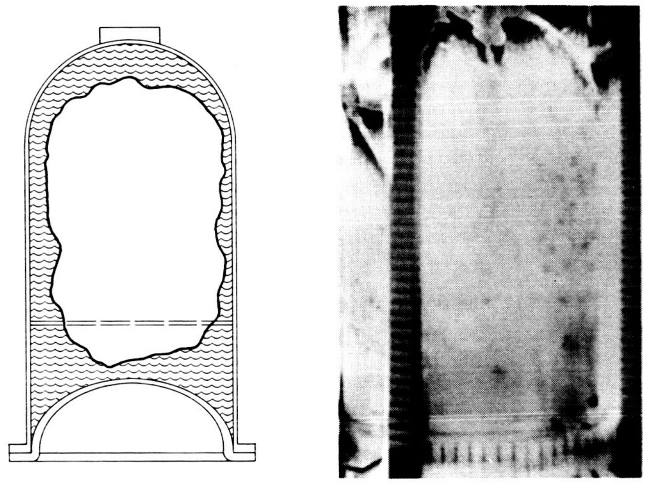

(b) Liquid at top of tank and displaced along tank walls.

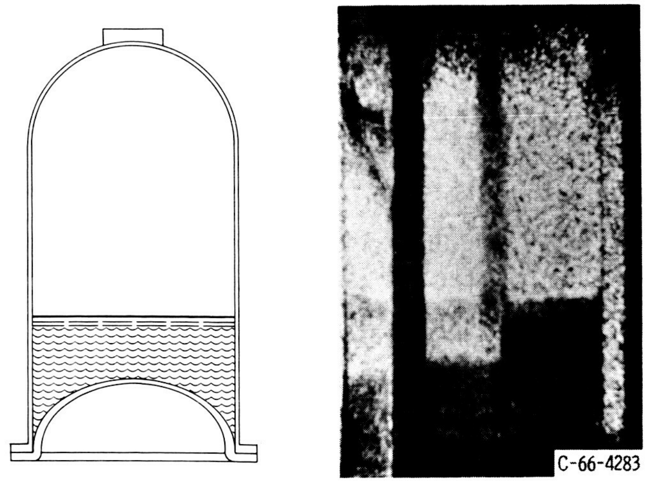

(c) Configuration of liquid-vapor interface after liquid reorientation.

Figure 16. - Turbulence occurring at beginning of experiment at longitudinal acceleration of 6.5×10^{-3} g.

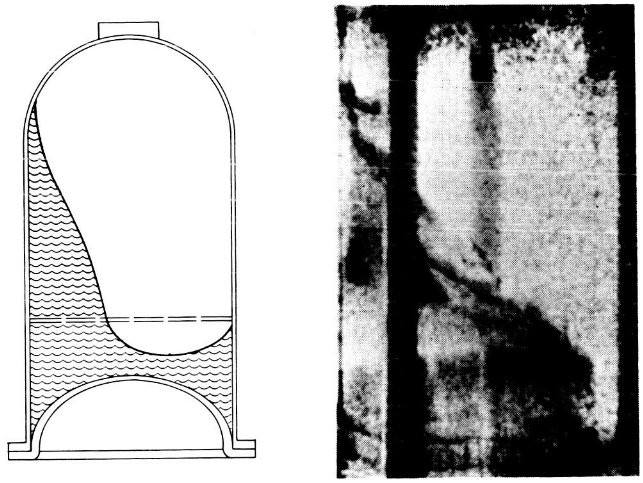

(a) Initial liquid slosh.

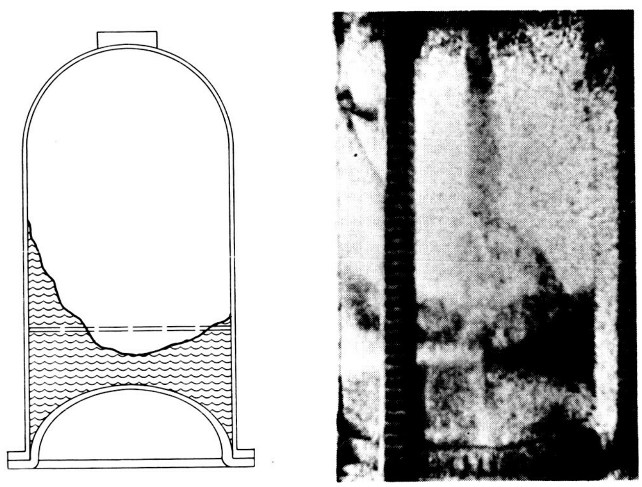

(b) Liquid slosh during first one-quarter cycle.

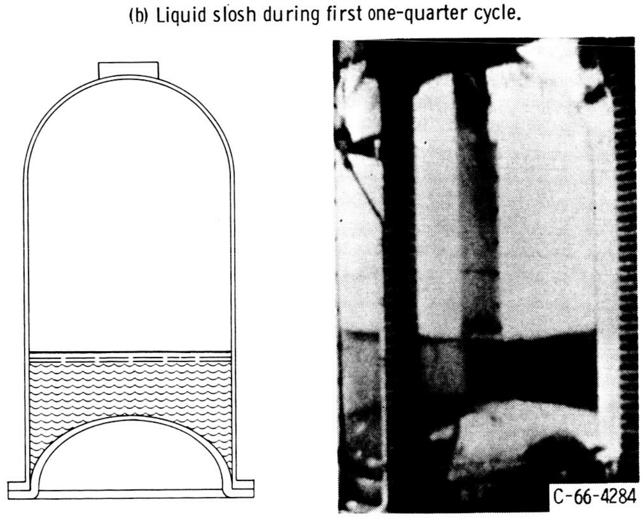

(c) Liquid at end of first one-quarter cycle.

Figure 17. - Liquid behavior during slosh at longitudinal acceleration of 6.5×10^{-3} g.

Slosh dynamics at longitudinal acceleration of 6.5×10^{-3} g. - An initial slosh wave, with an amplitude of sufficient magnitude to cause the wave to impinge on the top of the tank, resulted from the 5-second application of 7×10^{-3}-g lateral acceleration. The effectiveness of the slosh baffle in damping this severe slosh wave was evident in that only one-quarter cycle of longitudinal thrust was required to reduce the slosh wave to essentially zero amplitude. Because the slosh wave was overdamped, natural frequency and damping ratio were not obtained. Shown in figure 17 (p. 23) are several television frames that illustrate the position of the liquid during and at the end of the damping cycle. The time taken to reach essentially the configuration shown in figure 17(c) from turnoff of the lateral thrustor was of the order of 20 seconds.

Slosh dynamics at longitudinal acceleration of 7.3×10^{-4} g. - The pictures obtained in each of the three slosh tests that were run at the 7.3×10^{-4} g longitudinal acceleration in-

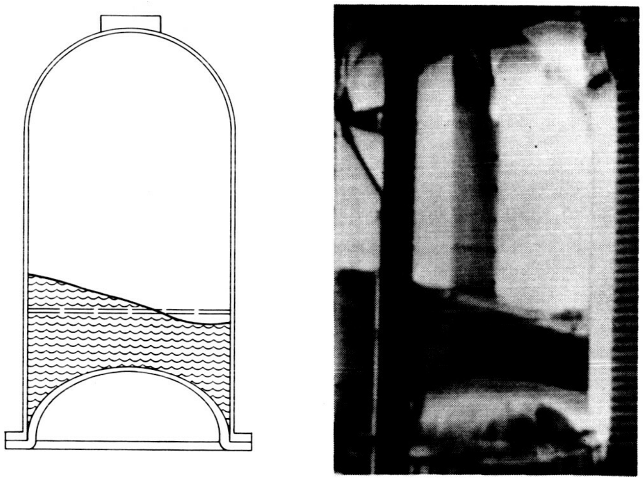

(a) Initiation of slosh wave.

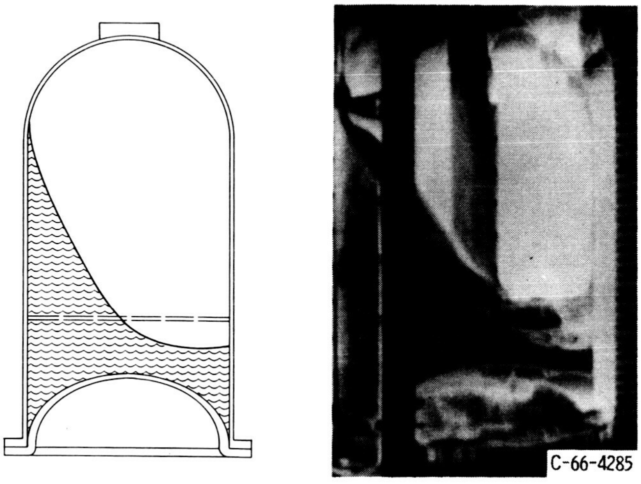

(b) Initial slosh at termination of lateral acceleration.

Figure 18. - Typical initial liquid slosh at longitudinal acceleration of 7.3×10^{-4} g.

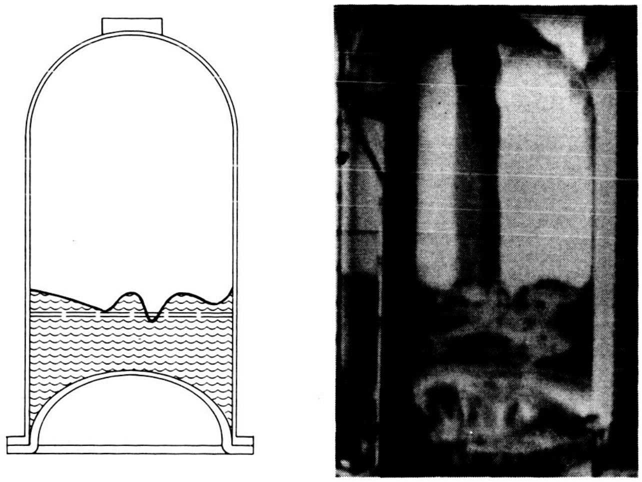

(a) Liquid slosh during first one-quarter cycle.

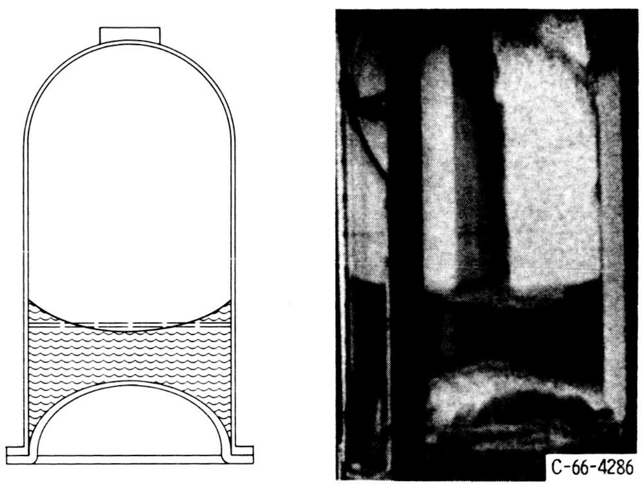

(b) Liquid at end of first one-quarter cycle.

Figure 19. - Typical liquid behavior during slosh at longitudinal acceleration of 7.3×10^{-4} g.

dicated nearly identical liquid behavior. Because of the high-amplitude-induced slosh obtained during the first test, an attempt was made by ground command to reduce the application time of the lateral acceleration. However, because of limitations of the command system, the shortest time of lateral thrust obtained was 2 seconds, which still caused the liquid to impinge on the top of the tank. A television frame that illustrates the initial slosh that is typical of this series is shown in figure 18. The effectiveness of the slosh baffle in damping this severe slosh wave is again evident in that only one-quarter cycle of longitudinal thrust was required to reduce the amplitude to essentially zero. Shown in figure 19 are typical television frames that illustrate the liquid position during and at the end of the damping cycle. The time taken to reach essentially the configuration shown in figure 19(b) from turnoff of the lateral thrustor did not exceed 30 seconds at this longitudinal acceleration level.

CONCLUDING REMARKS

A liquid slosh experiment, performed in a ballistic rocket flight, demonstrated that in a cylindrical tank slosh damping induced by a ring-type baffle was sufficient to damp slosh in less than one-quarter cycle at longitudinal settling accelerations of 6.5×10^{-3} and 7.3×10^{-4} g. The two-stage launch vehicle provided a period of over 6 minutes above 250 000 feet for the 1528-pound payload and performed very close to design values on this, its first, flight.

Lewis Research Center,
National Aeronautics and Space Administration,
Cleveland, Ohio, November 1, 1966,
124-09-03-01-22.

REFERENCES

1. Masica, William J.; Derdul, Joseph D.; and Petrash, Donald A.: Hydrostatic Stability of the Liquid-Vapor Interface in a Low-Acceleration Field. NASA TN D-2444, 1964.
2. Crabill, N. L.: Ascent Problems of Sounding Rockets. AGARD Rep. No. 391, July 1961.
3. James, Robert L., Jr.; and Harris, Ronald J.: Calculation of Wind Compensation for Launching of Unguided Rockets. NASA TN D-645, 1961.

NASA-Langley, 1967 —— 31 E-3636